

## Supplementary Materials for

### **Deciphering molecular and cellular *ex vivo* responses to bispecific antibodies**

#### **PD1-TIM3 and PD1-LAG3 in human tumors**

Marina Natoli\*, Klas Hatje, Pratiksha Gulati, Fabian Junker, Petra Herzig, Zhiwen Jiang, Iakov I. Davydov, Markus Germann, Marta Trüb, Daniel Marbach, Adrian Zwick, Patrick Weber, Stefan Seeber, Mark Wiese, Didier Lardinois, Viola Heinzelmann-Schwarz, Robert Rosenberg, Lothar Tietze, Kirsten D. Merz, Pablo Umaña, Christian Klein, Laura Codarri-Deak, Henry Kao\* and Alfred Zippelius\*.

\*Corresponding authors. Email: [marina.natoli@unibas.ch](mailto:marina.natoli@unibas.ch), [alfred.zippelius@usb.ch](mailto:alfred.zippelius@usb.ch), [henry.kao@roche.com](mailto:henry.kao@roche.com)

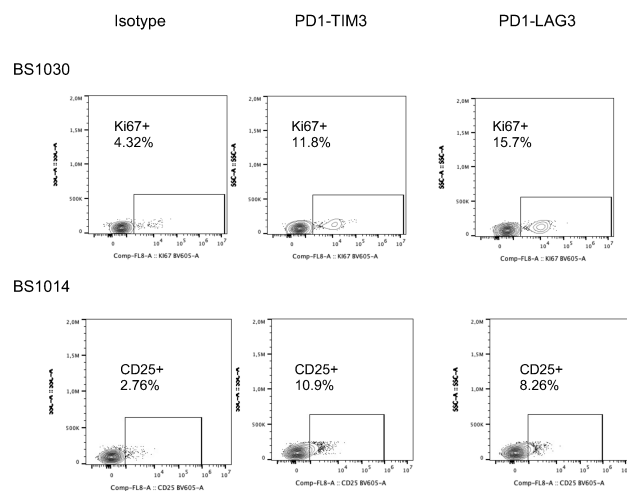
#### **This file includes:**

Figs. S1 to S7

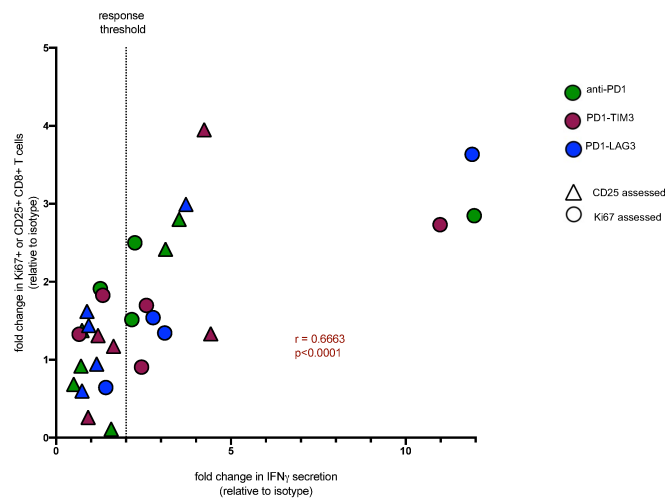
Tables S1 to S6

References (1 to 3)

**A**



**B**



**C**

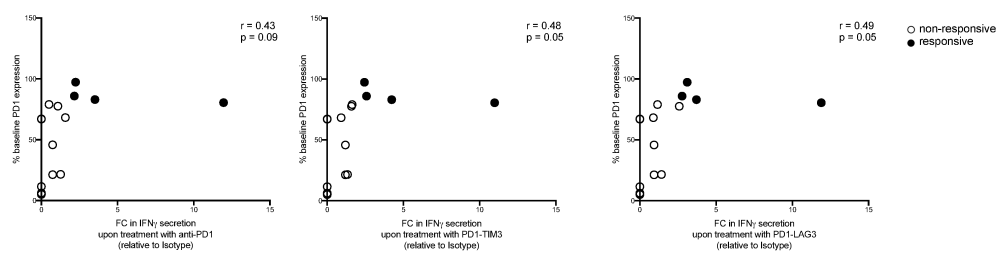
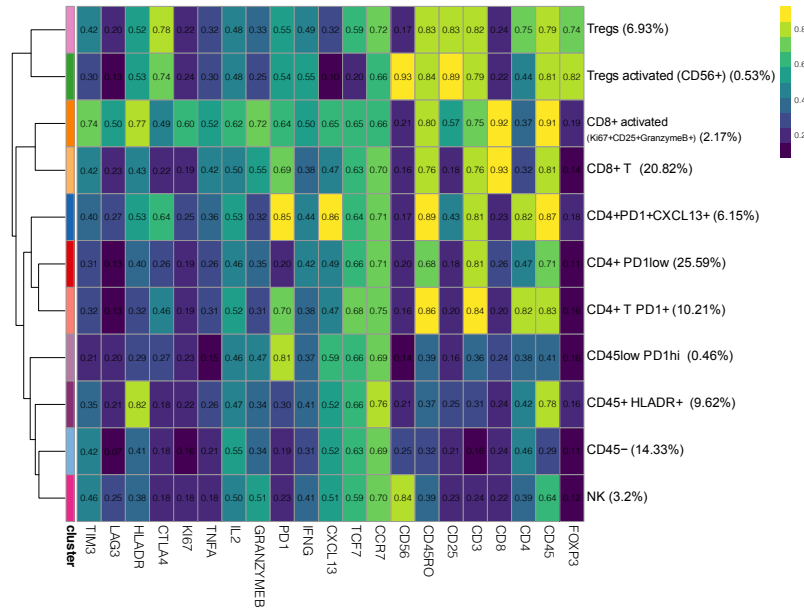


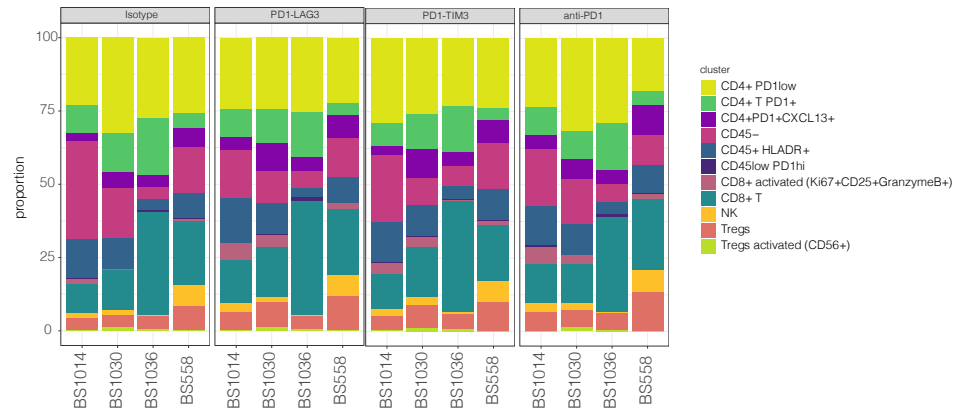
**Fig. S1.**

(A) Representative dot plots showing expression of Ki67 or CD25 on CD8<sup>+</sup> T cells from patients BS1030 or BS1014 tumor suspension in indicated treatment conditions. (B) Correlation between fold change in IFN- $\gamma$  secretion and fold change in activated CD8<sup>+</sup> T cells (according to either Ki67 or CD25 expression), comparing each treated sample (n of patients=11, color-coded by treatment) to the isotype control. Correlation coefficient  $r$  and  $p$  value are indicated (spearman's correlation). (C) Linear correlation of the fold change (FC) in IFN- $\gamma$  secretion induced by each compound and the baseline PD-1 expression in each tumor sample assessed (n= 16). Correlation coefficient ( $r$ ) and  $p$  value are indicated.

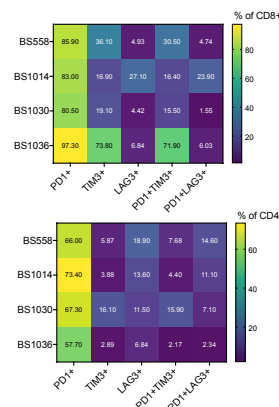
**A**



**B**



**C**



**D**

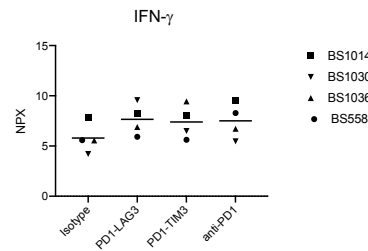




**Fig. S2.**

(A) Heatmap of the median (logicle-transformed) marker expression of lineage and functional markers across all cells analysed from pooled conditions clustered using *FlowSOM* and *ConsensusClusterPlus* and annotated. Color scale indicates the level of expression, dendograms indicate Euclidean distance metric and average linkage of cell types. (B) Per-patient bar plots indicating the proportion of each cell type in each treatment condition. (C) Heatmaps showing frequency of expression of PD1, TIM3, LAG3 and PD1/TIM3 or PD1/LAG3 co-expression on CD8<sup>+</sup> (top) or CD4<sup>+</sup> (bottom) T cells from the four indicated responsive patient tumor suspensions at the baseline. (D) NPX of IFNG (IFN- $\gamma$ ) measured by Olink technology in the supernatant of the four responsive tumor suspension across different treatment vs control comparisons.

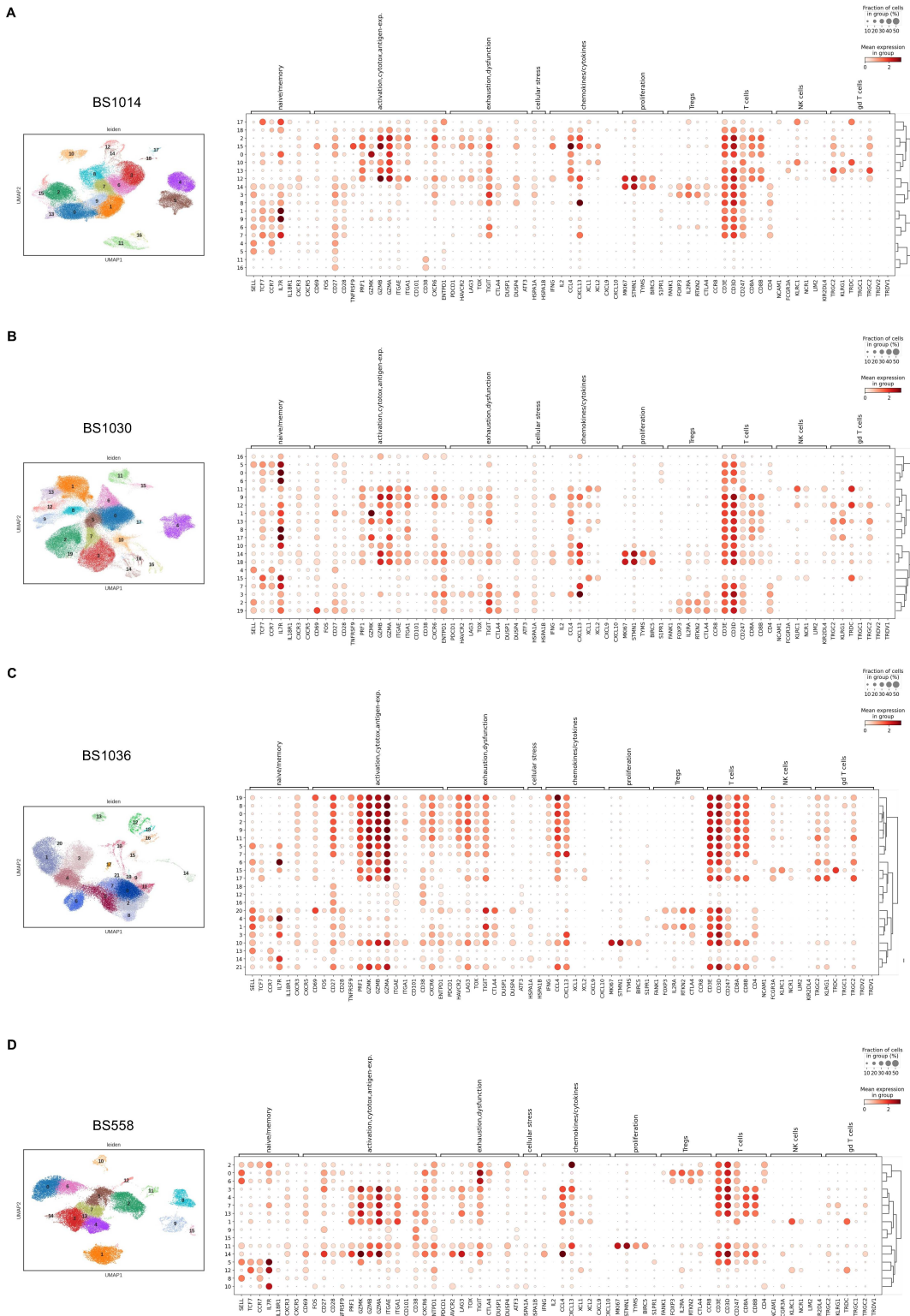


**Fig. S3.**

(A-D) Per-patient UMAP projections showing Leiden clustering from *Besca* standard workflow (left) and dot plots (right) showing mean expression and fraction of cells expression selected gene markers in each Leiden cluster, calculated by COSG (1).

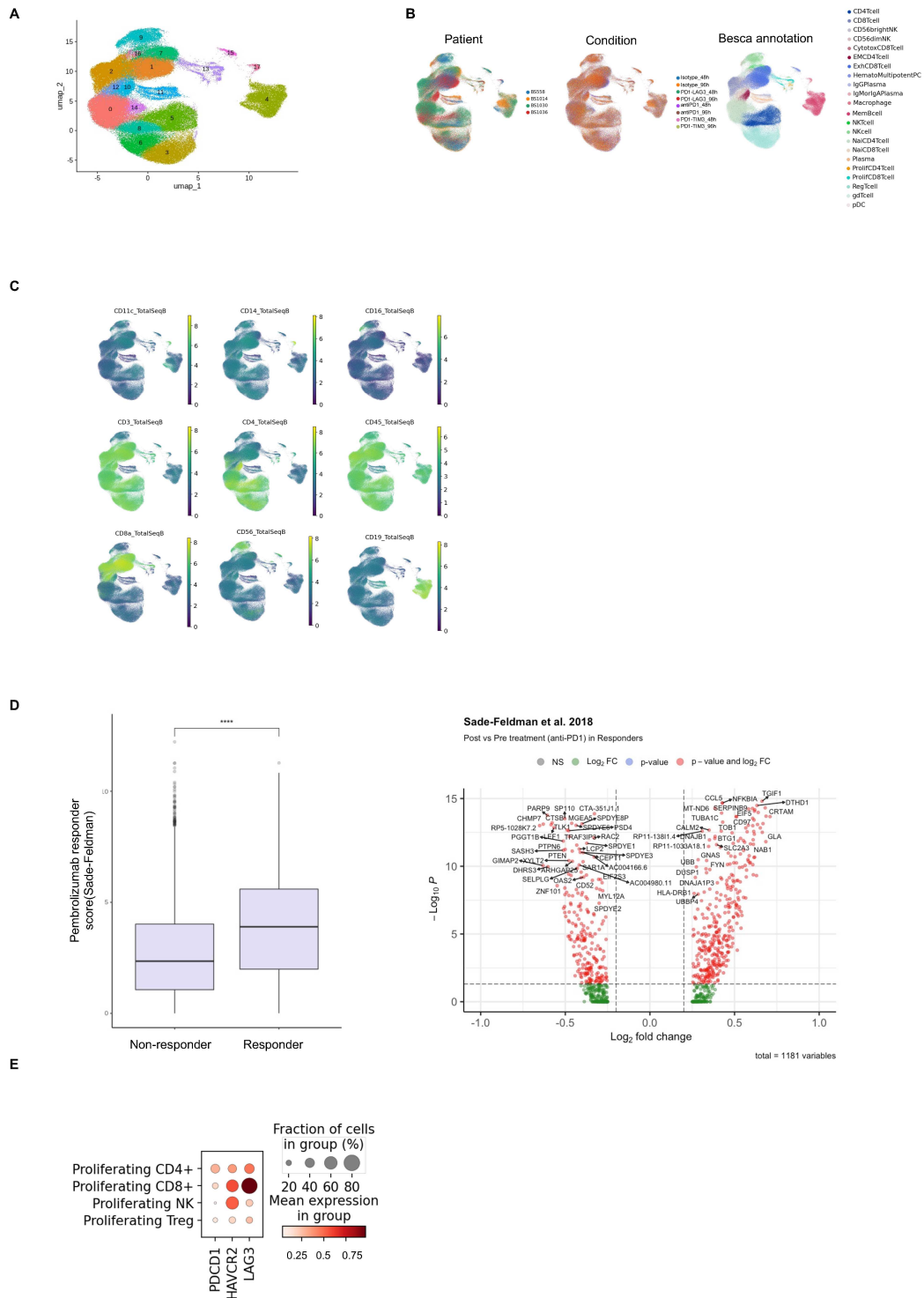


**Fig. S4.**

(A) UMAP projection showing Leiden clustering of merged and batched corrected (BBKNN) cells merged from all patients. (B) UMAP projections of final and merged scRNAseq dataset displaying cells belonging to either different patients (left) or conditions (treatment and timepoint; middle) and annotated using *Besca* automated cell labels. (C) UMAP projections showing the expression of Antibody-Derived Tags (ADT) from the CITE-seq library, confirming cell type annotation on a protein level. (D) Boxplots (left) showing a significant difference (Wilcoxon paired signed rank test) in the PD1 response score, calculated as described in the methods, between all cells derived from anti-PD1 non-responders and those deriving from anti-PD1 responders from the Sade-Feldman (2) dataset. Volcano plot showing differential expression of genes in responders to anti-PD1 from the Sade-Feldman (2) dataset, comparing pre and post treatment conditions. The genes were used to derive the anti-PD1 response score. (E) Dot plot showing mRNA expression of *LAG3*, *HAVCR2* and *PDCDI* in the different proliferating cell types from pooled conditions.

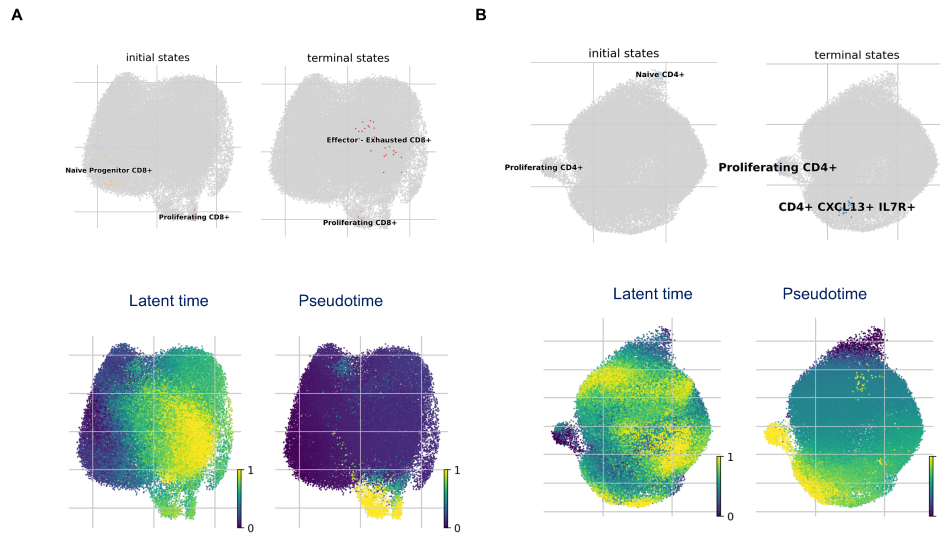


**Fig. S5.**

(A) UMAP of CD8<sup>+</sup> T cell subsets from pooled conditions (all treated cells from the 96 hour timepoint) with putative initial (up left) and terminal (up right) states, latent time (bottom left) and pseudotime (bottom right), calculated using *scVelo* (3). The latent time is a measure of transcriptional dynamics which accounts for speed and direction of motion, while the pseudotime indicates the distance between fates without recognising their temporal position (3). (B) UMAP of conventional CD4<sup>+</sup> T cell subsets from pooled conditions (all treated cells from the 96 hour timepoint) with putative initial (up left) and terminal (up right) states, latent time (bottom left) and pseudotime (bottom right) calculated using *scVelo* (3).

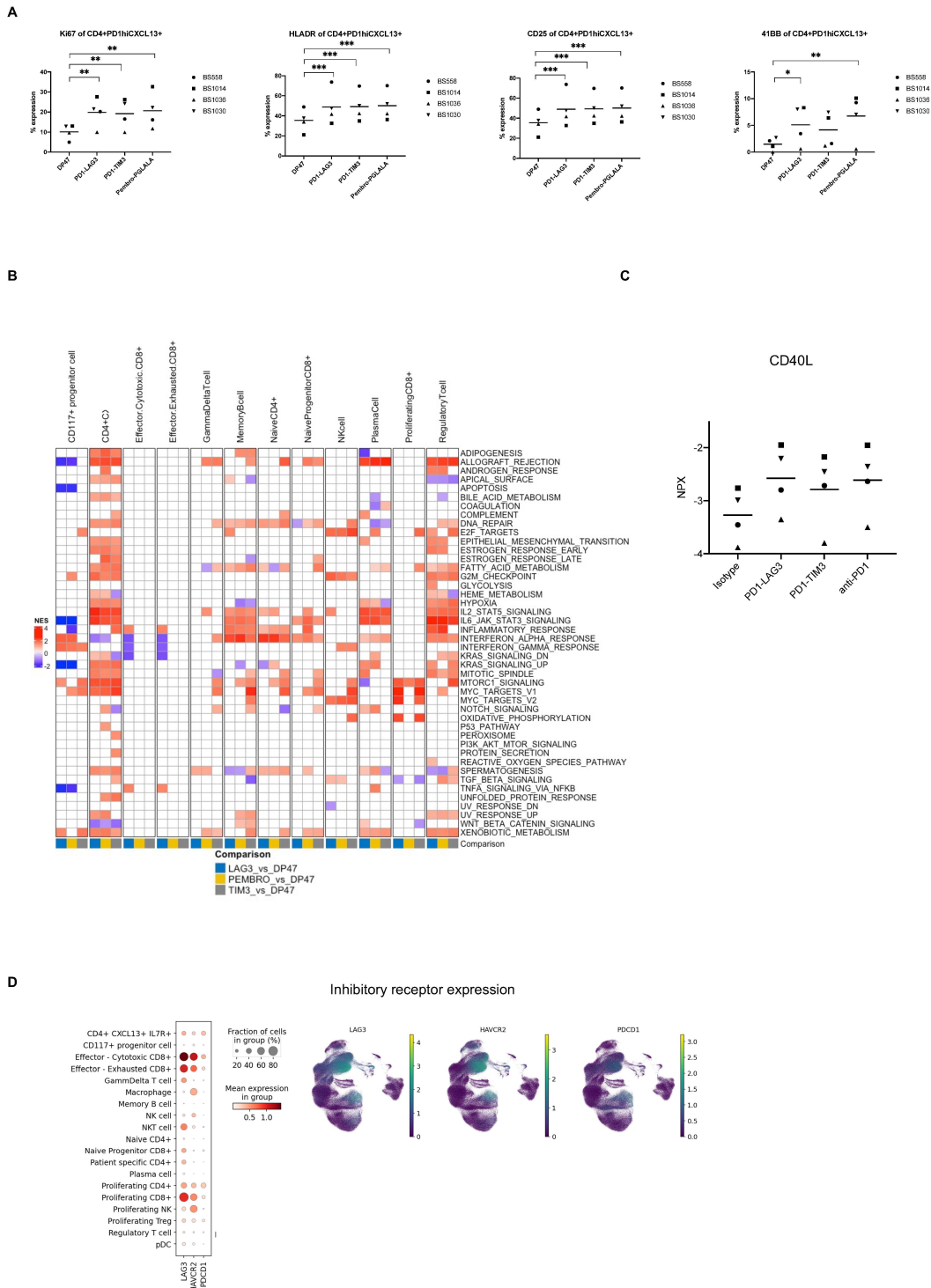


**Fig. S6.**

(A) Percentage expression of Ki67, HLA-DR, 41BB and CD25 on the CD4<sup>+</sup>PD1<sup>+</sup>CXCL13<sup>+</sup> population in the four responsive tumor suspension in different treatment conditions, manually gated, as shown in Figure S7B. (B) Heatmap of gene set enrichment analysis run on the pseudobulk outputs for each cell type, showing the normalized enrichment score (NES) for each Hallmark pathway within each cell type and comparison (treatment vs control, indicated in the colour legend at the bottom) at the 96 hour timepoint. Only pathways with significant enrichment are coloured (GSEA;  $p < 0.05$ ). (C) NPX of CD40L measured by Olink technology in the supernatant of the four responsive tumor suspension across different treatment vs control comparisons ( $FDR < 0.05$ ). (D) Dot plot (left) and UMAP projections (right) showing expression of *LAG3*, *HAVCR2* and *PDCD1* in the different annotated cell typed from pooled conditions. Dot plot (right) showing expression of known LAG3, PD1 and TIM3 ligands in the different annotated cell typed from pooled conditions.



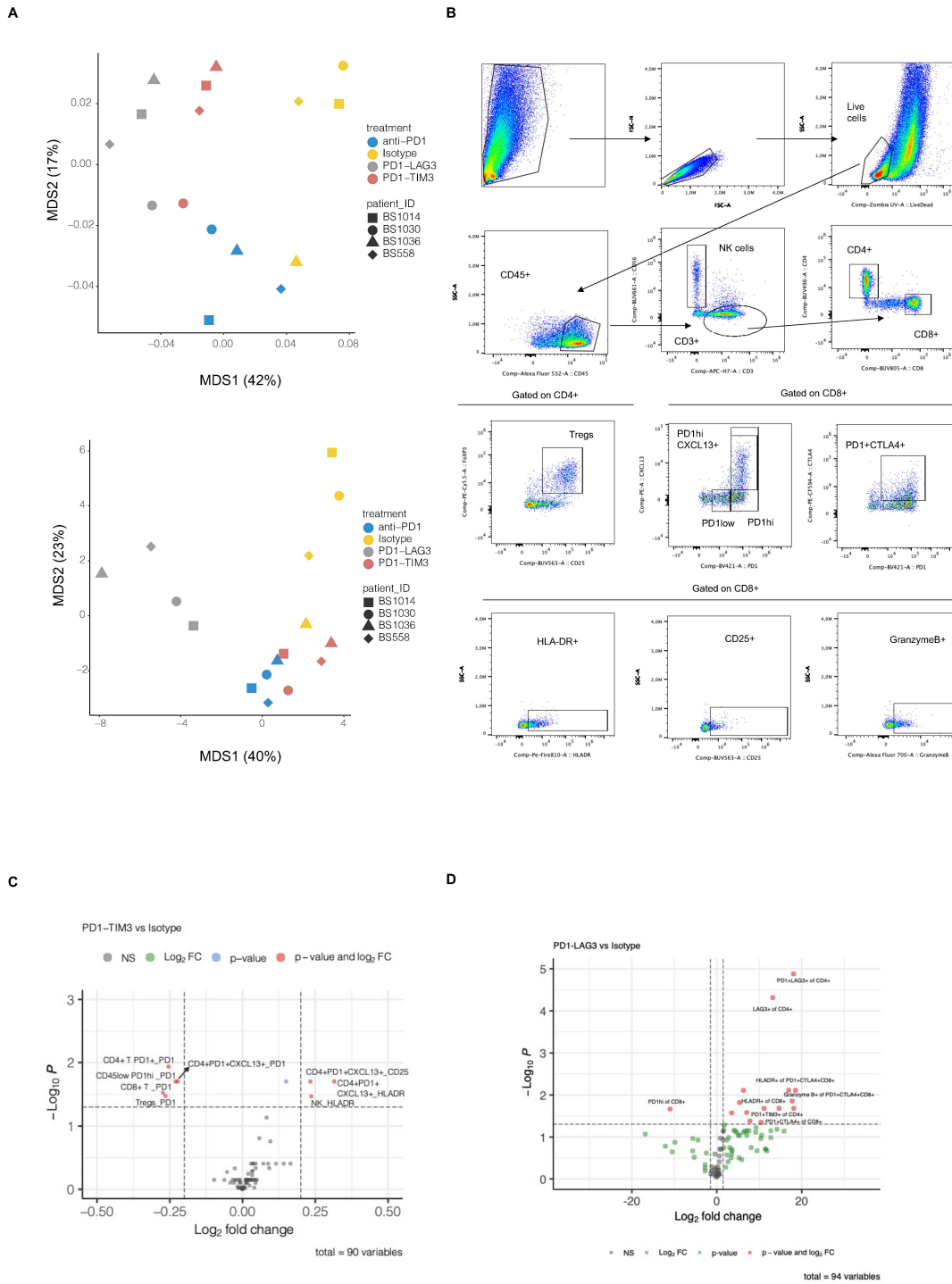


**Fig. S7.**

(A) Top: Multidimensional scaling plots of each indicated sample, based on the scaled and transformed fluorescence intensities of each marker on all cell populations and batch-adjusting by patient (using *ComBat* in R). Bottom: Multidimensional scaling plots of each indicated sample, based on manually gated frequencies of each marker on all cell populations, manually gated, and batch-adjusting by patient (using *ComBat* in R), indicating the distance in similarity between samples. (B) Representative schematic showing gating strategy for main lymphoid populations within tumor suspensions. (C) Volcano plot depicting differentially expressed markers ( $\log F_c > |1.5|$ , adjusted p value  $< 0.05$ ) within each cell subset across patients in the PD1-TIM3 treated condition compared to the isotype control. The colour legend indicates significant values according to the indicated thresholds. The values were obtained by running a linear mixed model using the median marker intensities of each population based on *FlowSOM* clustering. (D) Volcano plot depicting differentially expressed markers ( $\log F_c > |1.5|$ , adjusted p value  $< 0.05$ ) within each cell subset across patients in the PD1-LAG3 treated condition compared to the isotype control. The colour legend indicates significant values according to the indicated thresholds. The values were obtained by running a linear mixed model using the manually gated frequencies of each marker on each population.

**Table S1.**

List of patient sample characteristics and their functional response to treatment *in vitro*  
(b.d.=below detection limit; n.d.= not done; n.a.=not enough CD8+ events available).

Patient	Cancer type	Sample type	Log2 fold change in IFN $\gamma$ PD1-TIM3 vs Isotype	Log2 fold change in IFN $\gamma$ PD1-LAG3 vs Isotype	Log2 fold change in IFN $\gamma$ anti-PD1 vs Isotype	Fold change in CD25 expression PD1-TIM3 vs Isotype	Fold change in CD25 expression PD1-LAG3 vs Isotype	Fold change in CD25 expression anti-PD1 vs Isotype	Fold change in Ki67 expression PD1-TIM3 vs Isotype	Fold change in Ki67 expression PD1-LAG3 vs Isotype	Fold change in Ki67 expression anti-PD1 vs Isotype
BS-172	RCC	tumor digest	b.d.	b.d.	b.d.	n.d.	n.d.	n.d.	0.82	0.885	0.925
BS-199	NSCLC	pleural effusion	0.671574148	1.369012042	0.1213565	1.33333333	n.a.	2.41666667	n.d.	n.d.	n.d.
BS-202	NSCLC	pleural effusion	-0.125617866	-0.179031296	0.6561898	0.2605042	1.62064826	0.11044418	n.d.	n.d.	n.d.
BS-217	RCC	tumor digest	b.d.	b.d.	b.d.	n.d.	n.d.	n.d.	n.a.	n.a.	n.a.
BS-403	SKCC	tumor digest	b.d.	b.d.	b.d.	n.d.	n.d.	n.d.	n.a.	n.a.	n.a.
BS-494	SKCC	tumor digest	0.417478072	0.504463937	0.3403863	n.d.	n.d.	n.d.	1.827057	0.644351	1.910739
BS-558	EOC	tumor digest	1.367594543	1.471664348	1.1149857	n.d.	n.d.	n.d.	1.69657	1.540897	1.514512
BS-688	EOC	tumor digest	0.181769618	0.264774785	1.8074517	n.d.	n.d.	n.d.	n.a.	n.a.	n.a.
BS-796	EOC	tumor digest	b.d.	b.d.	b.d.	n.d.	n.d.	n.d.	1.121756	0.946108	1.047904
BS-899	EOC	tumor digest	-0.607082255	-0.436027921	-0.491414	1.32673267	0.59919028	0.91902834	n.d.	n.d.	n.d.
BS-965	NSCLC	tumor digest	b.d.	b.d.	b.d.	n.d.	n.d.	n.d.	n.a.	n.a.	n.a.
BS-969	EOC	tumor digest	0.715289174	0.214059572	-0.987113	1.17322835	0.94488189	0.68503937	n.d.	n.d.	n.d.
BS-988	NSCLC	tumor digest	0.260821334	-0.103274017	-0.430851	1.31174089	1.43894389	1.37623762	n.d.	n.d.	n.d.
BS-1014	NSCLC	tumor digest	2.081584019	1.892021427	1.814856	3.94927536	2.99275362	2.80072464	n.d.	n.d.	n.d.
BS-1030	NSCLC	tumor digest	3.457241008	3.572910327	3.5800249	n.d.	n.d.	n.d.	2.731481	3.634259	2.847222
BS-1036	Melanoma (metastasis)	tumor digest	1.289334823	1.634327435	1.1709954	n.d.	n.d.	n.d.	0.90625	1.34375	2.5
BS-1047	NSCLC	tumor digest	b.d.	b.d.	b.d.	n.d.	n.d.	n.d.	0.955437	1.003565	1.240642
BS-1054	NSCLC	tumor digest	b.d.	b.d.	b.d.	n.d.	n.d.	n.d.	0.843195	0.869822	1.142012
LA-062	CRC	tumor digest	b.d.	b.d.	b.d.	n.d.	n.d.	n.d.	n.a.	n.a.	n.a.
LI-005	CRC	tumor digest	b.d.	b.d.	b.d.	n.d.	n.d.	n.d.	1.141791	0.614179	1.186567
LI-043	CRC	tumor digest	b.d.	b.d.	b.d.	n.d.	n.d.	n.d.	n.a.	n.a.	n.a.

**Table S2.**Clinical information of patients and tumors used in *ex vivo* assays.

Patient ID	Date (MM/YYYY)	Sex	Age	Primary site	Histology	Type of specimen	Stage	Prior treatment	Subsequent treatment	Time from first diagnosis to relapse and/or progression (mo)	In vitro responsive (Yes or No)
BS-172	04/2013	male	67	kidney	clear cell carcinoma	primary	IV	none	votrient, radiotherapy	44	N
BS-199	07/2013	male	64	lung	adenocarcinoma	metastasis	IV	erlotinib, surgery	none	29	N
BS-202	07/2013	male	50	liver	pleomorphic carcinoma	metastasis	IV	none	none	2	N
BS-217	09/2013	male	39	kidney	clear cell carcinoma	primary	IV	none	temsirolimus, sunitinib, everolimus	7	N
BS-403	10/2019	female	67	skin	melanoma	metastasis	IV	extremity perfusion, radiotherapy, ipilimumab, surgery, DTIC, nivolumab	none	48	N
BS-494	01/2016	female	36	skin	melanoma	metastasis	IV	BRAF/MEK inhibitors, surgery, ipilimumab, radiotherapy, pembrolizumab, nivolumab	none	8	N
BS-558	06/2016	female	79	ovary	adenocarcinoma	primary	IV	chemotherapy	bevacizumab, chemotherapy	2	Y
BS-688	03/2017	female	47	ovary	adenocarcinoma	primary	III	none	chemotherapy, letrozol	in remission	N
BS-796	04/2018	female	62	ovary	adenocarcinoma	primary	III	none	chemotherapy	in remission	N
BS-899	03/2019	female	80	ovary	adenocarcinoma	primary	IV	chemotherapy	none	20	N
BS-965	10/2019	male	70	lung	squamous carcinoma	primary	I	none	none	in remission	N
BS-969	10/2019	female	43	ovary	adenocarcinoma	primary	IV	none	chemotherapy, bevacizumab, letrozol, olaparib	in remission	N
BS-988	01/2020	male	71	lung	squamous carcinoma	primary	III	none	chemotherapy	in remission	N
BS-1014	03/2020	female	45	lung	adenocarcinoma	primary	IV	none	chemotherapy, radiotherapy	7	Y
BS-1030	06/2020	male	68	lung	adenocarcinoma	primary	II	none	chemotherapy	in remission	Y
BS-1036	07/2020	male	55	skin	melanoma	metastasis	IV	ipilimumab, nivolumab	nivolumab	in remission	Y
BS-1047	08/2020	male	60	lung	adenocarcinoma	primary	III	none	chemotherapy	18	N
BS-1054	08/2020	male	70	lung	squamous carcinoma	primary	I	none	none	in remission	N
LA-062	07/2017	male	86	colon	adenocarcinoma	primary	I	none	none	in remission	N
LI-005	04/2019	male	78	colon	adenocarcinoma	primary	II	none	none	in remission	N
LI-043	03/2020	female	71	colon	adenocarcinoma	primary	III	none	none	in remission	N

**Table S3.**

Antibody panel for immunophenotyping of human tumor infiltrating lymphocytes from tumor suspensions.

<b>Fluorochrome</b>	<b>Marker</b>	<b>Type</b>
BUV395	CCR7	Lineage
BUV737	CD137	Functional
PE-CF594	CD152	Functional
BUV563	CD25	Lineage/Functional
APC-H7	CD3	Lineage
BUV496	CD4	Lineage
Alexa Fluor 532	CD45	Lineage
BV480	CD45RO	Lineage
BUV661	CD56	Lineage
BUV805	CD8	Lineage
PE	CXCL13	Functional
PECy5.5	FoxP3	Lineage
Alexa Fluor 700	Granzyme-B	Functional
Pe fire 810	HLA DR	Functional
BB700	IFN- $\gamma$	Functional
BV711	IL2	Functional
BV605	Ki67	Functional
FITC	LAG-3	Functional
BV421	PD-1	Functional
AF647	TCF7	Lineage/Functional
BV650	TIM-3	Functional
BV785	TNFA	Functional

**Table S4.**

List of significantly differentially expressed ( $p < 0.05$ ) markers on different populations comparing PD1-LAG3 to control isotype treatment. (Celltype\_marker indicates the celltype (before “\_”) on which each marker (after “\_”) is differentially expressed, AveExpr=average expression, logFC=log fold change, t=t statistic, adj.P.Val=adjusted p value).

Celltype_marker	logFC	AveExpr	t	P.Value	adj.P.Val
CD4+PD1+CXCL13+_LAG3	0.33333626	1.741619	7.396411	3.67E-06	0.00032996
CD4+PD1+_PD1	-0.2726836	3.03E+00	-5.628036	6.57E-05	0.00295588
Tregs_CD25	0.18925793	3.397877	5.172804	1.48E-04	0.00361943
CD8+ T_PD1	-0.3768561	2.86774	-5.126959	1.61E-04	0.00361943
CD4+PD1+CXCL13+_PD1	-0.2480212	3.497264	-4.89545	2.46E-04	0.00442931
CD4+PD1+CXCL13+_CD25	0.35976388	2.335802	4.747422	3.24E-04	0.00446514
CD4+PD1+CXCL13+_HLADR	0.26944116	2.195454	4.707644	3.49E-04	0.00446514
CD8+ T_LAG3	0.27364816	1.753019	4.639339	3.97E-04	0.00446514
Tregs_PD1	-0.3290556	2.597169	-4.479933	5.37E-04	0.00536541
CD45lowPD1hi_PD1	-0.254008	3.28E+00	-4.419475	6.02E-04	0.00541778
NK_HLADR	0.22610267	1.758442	3.376429	4.60E-03	0.03558052
Tregs_HLADR	0.26006525	2.117816	3.360846	4.74E-03	0.03558052
NK_IFNG	0.06685307	1.749416	3.22176	6.25E-03	0.0432322
CD4+PD1+CXCL13+_IFNG	0.06978501	1.800012	3.18435	6.73E-03	0.0432322
CD4+PD1+_HLADR	0.11646278	1.632634	3.128322	7.51E-03	0.04507382
Tregs_IFNG	0.08063878	1.852872	3.062117	8.56E-03	0.04815769
CD4+PD1+_LAG3	0.09984621	1.573094	2.998091	9.71E-03	0.05142509
CD4+PD1+CXCL13+_CXCL13	0.17999464	3.302121	2.936842	1.10E-02	0.05479409
CD45+HLADR+_HLADR	0.06441121	3.286862	2.872507	1.24E-02	0.05890787
Tregs_KI67	0.05246488	1.916739	2.767427	1.53E-02	0.06875757
Tregs_CXCL13	-0.3239322	1.282663	-2.57608	2.22E-02	0.09501202
CD4+PD1+CXCL13+_KI67	0.04906689	1.957157	2.512575	2.51E-02	0.10251616
CD45lowPD1hi_LAG3	0.10947494	1.666606	2.432141	2.92E-02	0.10854559
CD4+PD1low_GRANZYMEB	0.04620489	1.915792	2.430089	2.94E-02	0.10854559
Tregs_CTLA4	0.09390596	2.918667	2.416111	3.02E-02	0.10854559
NK_LAG3	0.05476046	1.593892	2.296616	3.78E-02	0.13095925
NK_KI67	0.05984958	1.889756	2.245442	4.17E-02	0.1388625
Tregs_LAG3	0.05685661	1.570189	2.216983	4.39E-02	0.13887352
CD8+ T_HLADR	0.08844332	1.831911	2.20725	4.47E-02	0.13887352

**Table S5.**

List of significantly differentially expressed ( $p < 0.05$ ) markers on different populations comparing PD1-TIM3 to control isotype treatment. (Celltype\_marker indicates the celltype (before “\_”) on which each marker (after “\_”) is differentially expressed, AveExpr=average expression, logFC=log fold change, t=t statistic, adj.P.Val=adjusted p value).

Celltype_marker	logFC	AveExpr	t	P.Value	adj.P.Val
CD4+PD1+_PD1	-0.2543429	3.03E+00	-5.249496	0.00012882	0.0115936
CD4+PD1+CXCL13+_PD1	-0.2229616	3.497264	-4.400823	6.24E-04	0.01984033
CD4+PD1+CXCL13+_CD25	0.31489129	2.335802	4.155286	1.00E-03	0.01984033
Tregs_CD25	0.14991551	3.397877	4.097496	1.12E-03	0.01984033
CD4+PD1+CXCL13+_HLADR	0.23285953	2.195454	4.068494	1.18E-03	0.01984033
CD45lowPD1hi_PD1	-0.2305264	3.28E+00	-4.01092	0.00132269	0.01984033
CD8+T_PD1	-0.2737894	2.87E+00	-3.724783	0.00231453	0.02975824
Tregs_PD1	-0.2643631	2.597169	-3.599176	2.96E-03	0.03333915
NK_HLADR	0.23637052	1.76E+00	3.52976	3.40E-03	0.03398195
NK_KI67	0.08230755	1.889756	3.088022	8.13E-03	0.0732115
CD8+T_CTLA4	0.05798453	1.47E+00	2.65671	1.90E-02	0.15513405
CD4+PD1+_HLADR	0.09498435	1.63E+00	2.551387	2.33E-02	0.1743966

**Table S6.**

Antibodies used for flow cytometry analyses.

Antibody	Fluorochrome	Clone / ID	Vendor	Cat. No
CD137	BUV737	4B4-1	BD Biosciences	741861
CD223	FITC	17B4	LS Bio	LS-B2237-50
CD25	BUV563	2A3	BD Biosciences	612919
CD3	APC-H7	Sk7	BD Biosciences	560275
CD4	BUV496	SK3	BD Biosciences	612936
CD45	AF532	HI30	Invitrogen	58-0459-42
CD45RO	BV480	UCHL-1	BD Biosciences	566192
CD56	BUV661	NCAM16.2	BD Biosciences	750478
CD8	BUV805	SK1	BD Biosciences	564912
CXCL13	PE	53610	RnD systems	IC801P
FoxP3	Pe-Cy5.5	PCH101	Invitrogen	35-4776-41
Goat anti-rabbit IgG	BV421	Poly1270	BD Biosciences	565014
Granzyme B	AF700	QA16A02	BioLegend	372222
HLADR	PeFire810	mIH1	BioLegend	custom
IFN- $\gamma$	BB700	B27	BD Biosciences	566395
IL-2	BV711	MQ1-17H12	BioLegend	500345
Ki67	BV605	Ki-67	BioLegend	350522
Live dead	Zombie UV	none	BioLegend	423108
Live dead	Zombie Aqua	none	BioLegend	423102
PD1	none	D4W2J	Cell Signaling Technology	86163
TCF7	AF647	7f11a10	BioLegend	655204
TNF $\alpha$	BV785	MAb11	BioLegend	502947



**Data file S1. (included as a separate file)**

Summary of sequencing statistics before quality check and filtering.

**Data file S2. (included as a separate file)**

scRNAseq cluster annotation table for each patient.

**Data file S3. (included as a separate file)**

Pseudo-bulk analysis output listing differentially expressed genes in each treatment to control comparison and in each cell type from scRNAseq dataset. Clusters were included in the analyses only when sufficient numbers of cells were present to allow for all treatment-control comparisons.

## References

1. M. Dai, X. Pei, X. J. Wang, Accurate and fast cell marker gene identification with COSG. *Brief Bioinform* **23**, (2022).
2. M. Sade-Feldman, K. Yizhak, S. L. Bjorgaard, J. P. Ray, C. G. de Boer, R. W. Jenkins, D. J. Lieb, J. H. Chen, D. T. Frederick, M. Barzily-Rokni, S. S. Freeman, A. Reuben, P. J. Hoover, A. C. Villani, E. Ivanova, A. Portell, P. H. Lizotte, A. R. Aref, J. P. Eliane, M. R. Hammond, H. Vitzthum, S. M. Blackmon, B. Li, V. Gopalakrishnan, S. M. Reddy, Z. A. Cooper, C. P. Paweletz, D. A. Barbie, A. Stemmer-Rachamimov, K. T. Flaherty, J. A. Wargo, G. M. Boland, R. J. Sullivan, G. Getz, N. Hacohen, Defining T Cell States Associated with Response to Checkpoint Immunotherapy in Melanoma. *Cell* **175**, 998-1013 e1020 (2018).
3. V. Bergen, M. Lange, S. Peidli, F. A. Wolf, F. J. Theis, Generalizing RNA velocity to transient cell states through dynamical modeling. *Nat Biotechnol* **38**, 1408-1414 (2020).